CONFERENCE PRE-PRINT

SIMULATION OF DEUTERIUM-TRITIUM ISOTOPE EFFECTS ON THE DIVERTOR TARGET HEAT FLUX DENSITY IN CFEDR

Chen Zhang*
School of Physics,Dalian University of Technology
Dalian, China
Email:zhangchen2013@dlut.edu.cn

Chaofeng Sang*
School of Physics,Dalian University of Technology
Dalian, China
Email:sang@dlut.edu.cn

Yu Bian, Xuele Zhao，Dezhen Wang
School of Physics,Dalian University of Technology
Dalian, China

Rui Ding, Xiaoju Liu
Institute of Plasma Physics, Chinese Academy of Sciences
Hefei, China

Abstract

The China Fusion Engineering Demonstration Reactor (CFEDR) deuterium-tritium (D-T) discharge is an important step for chinese nuclear fusion energy. With the fusion power of several gigawatts in CFEDR, the divertor target will face significant challenges in heat flux deposition (q_t). However, the D-T isotope effect can cause differences in transport and collisions of plasma in the scrape-off layer and divertor, which could affect neutral radiation in divertor region, as well as heat flux decay length (λ_q), thereby affecting q_t. In this work, we investigate the isotope effects of q_t on CFEDR using SOLPS-ITER modeling, and the simulation results agree with previous D-T simulation from the JET-ILW. The midplane pedestal density in the equal-proportion D-T discharge is higher than that in the pure deuterium (D) discharge, with a smoother n_e gradient near the separatrix and a larger λ_q. In D-T discharge conditions, both the T_e and q_t are slightly lower compared to the D discharge. In divertor region, distinct differences are observed near the target: both T+ and T show stronger accumulation close to the target compared to D^+ and D, while the n_D and n_{D+} are higher in regions farther from the target. It could be explained by the recycled atomic and charge-exchange collision, which can process further increases the energy of D atoms in the divertor than that of T, making D neutral more likely transport to far from the target areas and be ionized. This results in an increase in T neutral particle density and energy losses of the plasma in the divertor region, resulting in T_e and q_t decrease in D-T discharge.

1. INTRODUCTION

CFEDR will use deuterium-tritium (D-T) as its fusion fuel. During its operation, the energy and helium (He) ash generated by fusion reactions need to be exhausted. The divertor is the main component of the fusion device that comes into contact with plasma. The high-energy flux and particle flux flowing out of the core may damage the target, posing a major challenge to its service life. Additionally, impurities produced by target erosion may enter the core plasma and disrupt the normal operation of the device.Tungsten is regarded as the primary plasma-facing material for divertor target. During steady-state discharges, to ensure the tungsten target remains undamaged, it is necessary to control the target electron temperature $T_{e,target}$ to be less than 10 eV and the steady-state deposited heat flux density $q_{t,target}$ to be below 15 MW/m² [1].The total fusion power designed for CFEDR is 1–3 GW, and the energy flux flowing into the scrape-off layer (SOL) is as high as 200–600 MW [2]. If the $q_{t,target}$ is not controlled, it will reach ten times the target thermal load limit, leading to divertor damage. Therefore, how to control the $q_{t,target}$ during discharge is one of the most critical physical issues.

Compared with pure deuterium discharges, the scrape-off layer (SOL) plasma transport and distribution exhibit different phenomena in D-T discharges. This results from the differences in ion gyroradius between D and T, as

well as the differences in thermal force and viscous force acting on D and T in the SOL [3]. Additionally, the differences in relevant collision reactions of D and T (such as ion-neutral charge exchange and neutral particle ionization, which also have different reaction cross-sections) and recycling coefficients contribute to the differences in fuel neutral particle distribution and radiation, thereby affecting $q_{t,target}$. Due to the high cost and radioactivity of tritium, only a limited number of D-T experiments have been conducted worldwide, specifically on the TFTR[4] and the JET[5]. In these experiments, it was observed that compared with pure deuterium discharges, the plasma distribution in the pedestal region during D-T discharges is flatter i.e. with a larger λ_q [6][7]. However, the erosion of the first wall and divertor remains a significant issue[5]. In the D-T experiments on JET-ILW, $q_{t,target}$ was reduced by increasing the injection rate of fuel gas, which alleviated impurity accumulation[5]. Nevertheless, excessive fuel gas injection leads to a decrease in core confinement performance and affects discharge stability.

The large-scale 2D edge plasma code SOLPS-ITER [8] is one of the most widely used edge plasma codes internationally. It can simulate edge plasma under different discharge conditions of real tokamaks, taking into account the effects of collisions, radiation, drifts, and transport of neutral particles and impurities on the edge plasma. SOLPS-ITER can also consider differences in force, and collision of plasma at the edge under isotope effects, enabling simulation studies on isotope plasma. S.O. Makarov et al. conducted preliminary simulation work on the D-T discharge experiment of JET-ILW using SOLPS-ITER, investigating the distribution of edge D-T plasma in the pedestal and divertor target under a 1:1 fuel injection ratio [9][10]. The simulation results show that D-T ions exhibit separated distributions in the divertor region: T atoms accumulate more near the target than D atoms, and the $q_{t,target}$ on the target is lower than that of pure D plasma. Li *et al.* used SOLPS-ITER to investigate the impact of the hydrogen isotope effect on divertor detachment in EAST. The simulation results show that with an increase in the fuel gas injection rate, T achieves detachment first at a lower fuel injection rate than that of D. However, in future large-scale fusion devices (such as ITER and CFEDR), the impact of the isotope effect on the divertor target plasma remains unknown. Therefore, it is of great importance to conduct simulation work on this issue. This study conducts simulation studies on CFEDR discharges using SOLPS-ITER, focusing on differences in $q_{t,target}$ on the different deuterium-tritium (D-T) injection ratios, and further discusses differences in the distribution of deuterium-tritium (D-T) plasma and neutral particles.

2. SIMULATION SETUP

In the current scenario design of CFEDR, the magnetic equilibrium adopts a lower single-null divertor configuration [2]. This divertor is installed in the lower part of the vacuum vessel, whose core function is to handle the heat and particles exhausted from the core plasma.Taking into account the layout constraints of poloidal field coils, the structural requirements of the blanket, and the available space conditions, both the inner and outer divertors adopt a traditional V-shaped geometric design (see Fig. 1 for its specific geometry and calculation mesh). Among them, the angle between the vertical target and the sloped target is 55° for the inner divertor, and 58° for the outer divertor. To further increase the divertor volume and enhance radiation in the outer divertor region, the leg length L_{leg} of the divertor has been optimized in the design: the outer divertor leg length is approximately 1.6 m, and the inner divertor leg length is about 1.4 meters. As shown in Table 1, the outer divertor leg length of CFEDR is similar to that of the reference design for the CFETR, and is 1.6 times longer than that of the ITER.Notably, unlike the designs of ITER and CFETR, the strike point of the CFEDR outer divertor is located on the sloped target rather than the vertical target， and the pumping slot is uniformly placed at the bottom of the divertor.

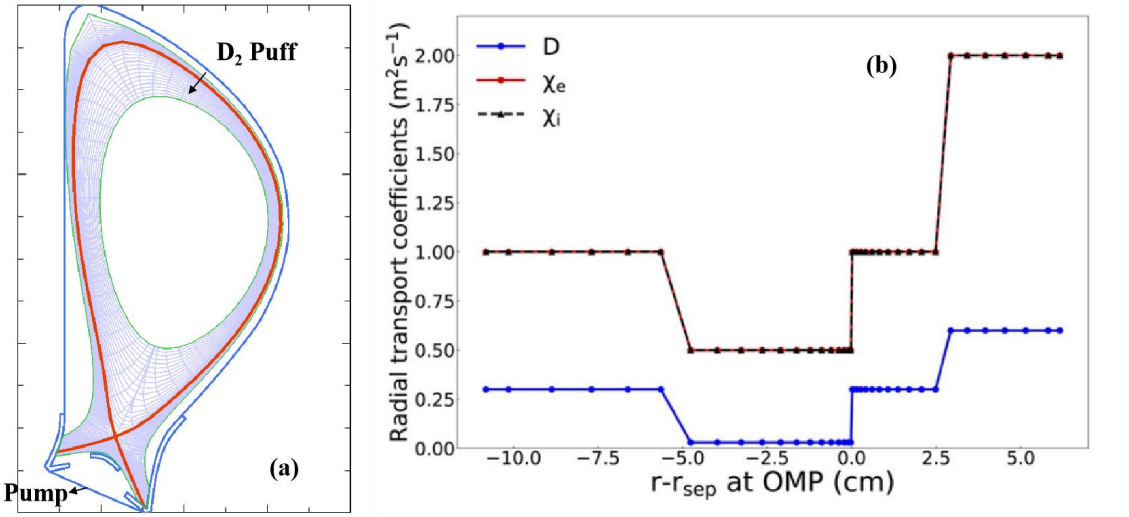

FIG.1 Divertor geometry and modeling mesh of CFEDR for SOLPS-ITER.

In this work, the SOLPS-ITER code package (3.0.9 version) , a coupled version of the multi-fluid transport code B2.5 and the kinetic neutral transport code EIRENE. The ions and electrons are simulated by B2.5, and the neutral particles are tracked in triangular meshes by EIRENE. SOLPS-ITER including full drifts and isotope effect. The computational mesh as shown in figure 1, is produced based on the standard CFEDR equilibrium with a toroidal magnetic field B_t = 6.3 T and plasma current I_p = 15 MA. The resolution of the simulation mesh is 96×36. The simulation domain ranges from the core–edge interface (CEI) to the at OMP, i.e. $r - r_{sep} \subset$ (−30.0, +6.8 cm) at outer mid-plane OMP. The input power P_{in} = 250 MW and the power is divided equally between electrons and ions [34, 35]. In the simulation, the recycling coefficient R_{rec} is set to 1 except for the pumping port, where *R*rec is set to 0.9925 (pumping speed ~ 200 L/s), and drift is taken into consideration and the direction of B×∇B drift points to X-point.[33]. The pedestal for H-mode is established by imposing the radial particle and heat transport coefficients. The radial transport coefficients are set as: D+ and T^+ particle transport coefficient $D_\perp$ = 0.3 m^2 s^{-1}, electron and ion heat conductivity coefficients $\chi_{\perp,e} = \chi_{\perp,i}$ = 1.0 m^2 s^{-1} in the core region, and a radial transport barrier is imposed by reducing $D_\perp$ = 0.03 m^2 s^{-1}, $\chi_{\perp,e} = \chi_{\perp,i}$ = 0.5 m^2 s^{-1} in the pedestal region, $D_\perp$ = 0.3 m^2 s^{-1} and $\chi_{\perp,e} = \chi_{\perp,i}$ = 1.0 m^2 s^{-1} at the outer near SOL, and $D_\perp$ = 0.6 m^2 s^{-1} and $\chi_{\perp,e} = \chi_{\perp,i}$ = 2.0 m^2 s^{-1} at the far SOL, which are the same as the previous CFEDR simulations[2].

In the simulation, only D^+, D, D_2, T and T^+ are considered, the effect of tungsten (W) intrinsic impurity and He ash is not considered here. The particle and energy reflection coefficients, which are functions of incident energy and angle, are calculated by TRIM [36], The recycling rate can be expressed as $R_N(\varepsilon_0, \alpha) = N_D + 2N_{D2}/N_0$, where N_D is the number of reflected D or T atoms, N_{D2} is the number of thermal-released molecules from the PFMs, and N0 is the number of total incident particles. The particle reflection rate $R_N(\varepsilon_0, \alpha) = N_D/N_0$. The energy reflection coefficient R_E can be expressed as $R_E(\varepsilon_0, \alpha) = \frac{N\bar{\varepsilon}}{N_0\varepsilon_0}$, and the average energy of the reflected particles $\bar{\varepsilon} = \frac{R_E(\varepsilon_0,\alpha)}{R_N(\varepsilon_0,\alpha)}\varepsilon_0$. The angle of the reflected particle follows specular reflection, which is similar to previous SOLPS simulation [11]. The particle and energy reflection coefficients as functions of incident D and T energy ranging from 10^1-10^3 eV on W marterials are shown in Fig. 2 (a-b). It can be clearly seen that the D has higher energy R_N and R_E than those of T. The reactions considered by EIRENE are listed in table 1, including D and T atomic ionization collision, charge exchange, D_2 molecules ionization and dissociation, dissociative-ionization, dissociative-excitation, dissociation-recombination, and elastic collisions between ion and neutral particles. D and T have similar ionization and recombination cross-sections, but the charge-exchange of D is higher than that of T.

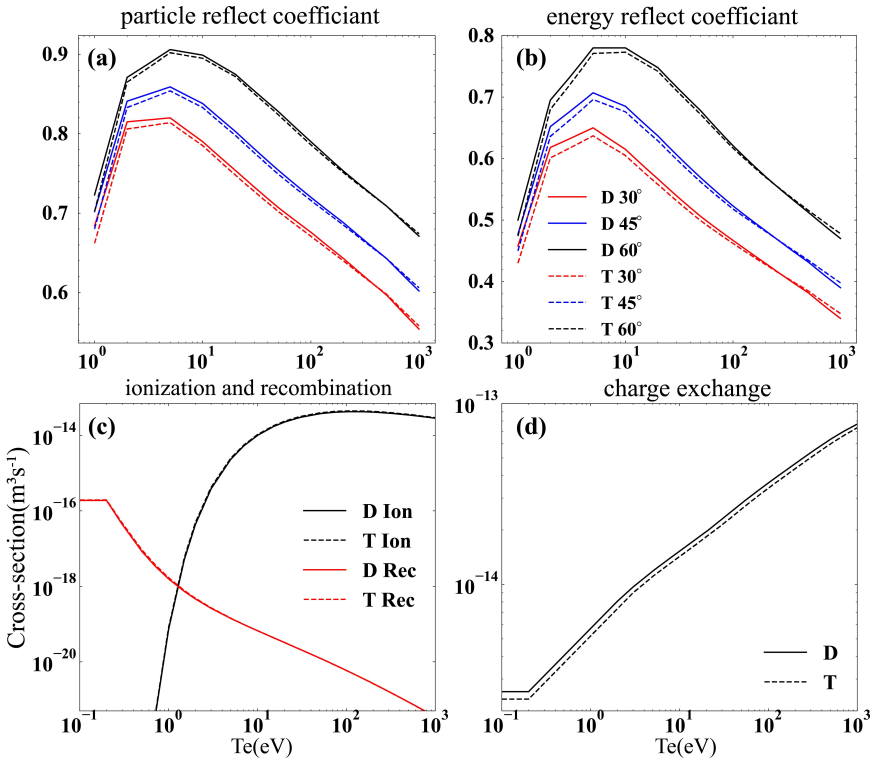

FIG.2 (a-b) Particle and Energy reflection coefficients, R_E for D and T at normal incidence (α=30,45,60) on W, (c-d) ionization and charge-exchange cross-section, as functions of incident energies ε_0 from 10^1~10^3 eV.

TABLE 1. The simulated collision reactions by Eirene.

Index	Reaction	Notation	Reaction type
1	$D + e \rightarrow D^+ + 2e$	AMJUEL H.4,10 2.1.5	Ionization[12][13]
2	$p + D(1s) \rightarrow D(1s) + p$	HYDHEL H.1,3 3.1.8	Charge-exchange[14]
3	$e + D_2 \rightarrow 2e + D^+$	AMJUEL H.4 2.2.9	Ionization[12][13]
4	$e + D_2 \rightarrow e + D + D$	AMJUEL H.4 2.2.5g	Dissociation[12][13]
5	$e + D_2 \rightarrow 2e + D + D^+$	AMJUEL H.4 2.2.10	Dissociative-ionization[12][13]
6	$p + D_2 \rightarrow p + D_2$	AMJUEL H.0,1,3 0.3	Elastic collision[13]
7	$p + D_2 \rightarrow D + D_2^+$	AMJUEL H.2 3.2.3	Ion conversion[13]
8	$e + D_2^+ \rightarrow e + D + D^+$	AMJUEL H.4 2.2.12	Dissociative-excitation[13]
9	$e + D_2^+ \rightarrow D + D$	AMJUEL H.4,8 2.2.14	Dissociation-recombination[13]
10	$e + D_2^+ \rightarrow 2e + D^+ + D^+$	AMJUEL H.4 2.2.11	Dissociative-ionization[13]
11	$p + e(s) \rightarrow D(1s) + ...$	AMJUEL H.4,10 2.1.8	Radiative recombination and three-body recombination [12][13]

3. MODELING AND DISCUSSION

3.1. The effect of D-T isotope on upstream and target plasma

In the simulation, the total net ion (D^+ and T^+) flux (Γ_{D+} and Γ_{T+}) at the core boundary (the innermost surface of the mesh) is assumed to be 5×10^{20} s^{-1}.Four cases are considered: pure D discharge (no external puffing);

D-T discharge with 1:1 proportional mixture (no external puffing); pure D discharge (D injected rate is 2×10^{22} s^{-1} from the upper puffing port); D-T 1:1 discharge with proportional mixture (both D and T injected rate is 1×10^{22} s^{-1} from the upper puffing port).

As shown in Figure 1(a), regardless of the presence of external puffing, the outer mid-plane (OMP) electron density ($n_{e,omp}$) of the D-T discharge is comparable to that of the pure D discharge at the core boundary, while it is larger at the separatrix (approximately 120% of that in the pure D discharge). This phenomenon is qualitatively consistent with both experiments and simulations of JET D-T discharges[6][7]. The simulation results also show that under D-T discharge conditions, the T^+ density is higher than the D^+ density in the pedestal region near the separatrix, while the opposite is true at the core boundary. The transport model of the SOL in the simulation is purely diffusive, without turbulent transport effects, and the plasma diffusivity is exactly the same across all operating conditions. Due to the smaller sound speed of T atoms, T is less likely to be transported to the core and accumulates at the boundary, which leads to the difference in $n_{e,omp}$ between the two types of discharges. The difference in the midplane electron temperature ($T_{e,omp}$) between different discharge conditions is smaller than that of $n_{e,omp}$ (Fig. 1(b)). Therefore, the wider λ_q under D-T discharge conditions is mainly caused by the gentler $n_{e,omp}$ gradient in its pedestal region.

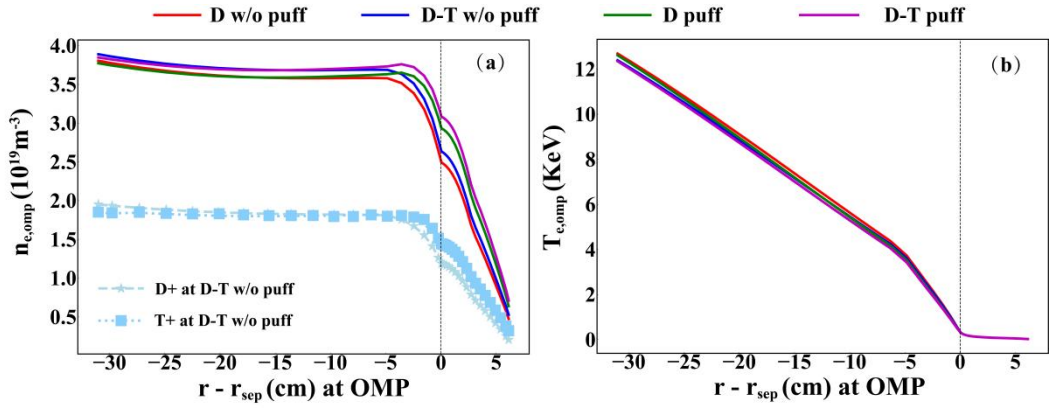

FIG.3 Profile of（a）$n_{e,omp}$ and（b）$T_{e,omp}$ at OMP in different discharge conditions

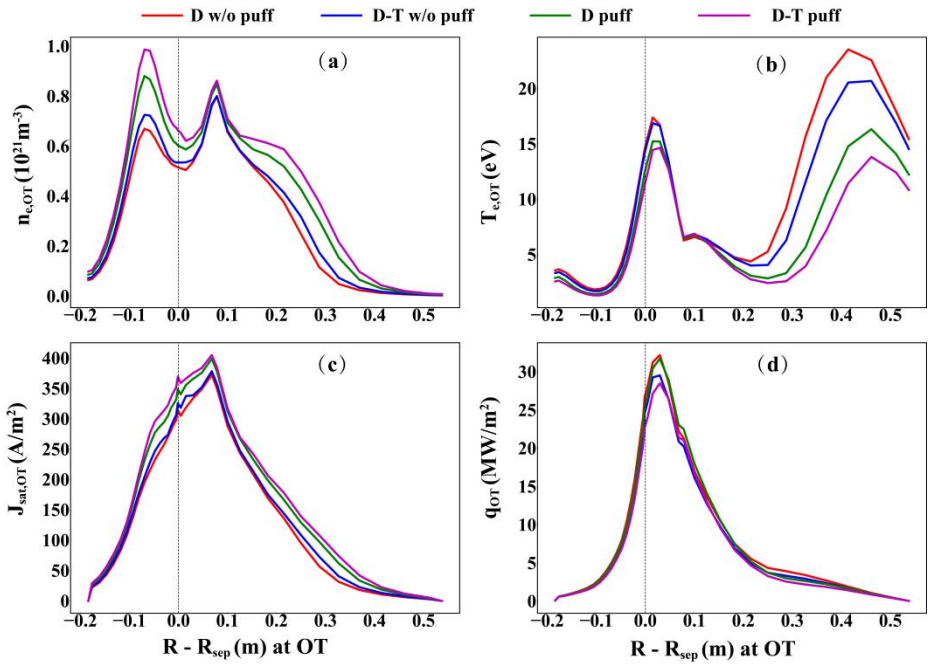

FIG.3 Profile of (a) $n_{e,OT}$, (b)$T_{e,OT}$ (c) $J_{sat,OT}$ and (d) q_{ot} at OT in different discharge conditions

Fig. 4 shows the plasma distribution at the outer divertor target (OT) under different discharge conditions. The simulation results indicate that fuel gas puffing at the upstream increases the $n_{e,ot}$ and the saturated ion current $J_{sat,ot}$, while effectively reducing $T_{e,ot,}$ i.e. under the gas puffing condition, $T_{e,ot}$ at the strike point and far SOL decreases by approximately 15% and 50% respectively compared with the non-puffing condition. And q_{ot} decreases by about 10%. Under the D-T discharge condition, $n_{e,ot}$ and $J_{sat,ot}$ increase by 20% and 10% respectively compared with the pure D discharge, while both $T_{e,ot}$ and q_{ot} decrease by 15%. This confirms that D-T discharge can effectively alleviate the high heat load challenge faced by CFEDR. Notably, when only pure D (or D-T) discharge is used without impurity seeding, the divertor remains in the attached condition, and q_{ot} far exceeds 15 MW/m². Therefore, it is still necessary to inject impurities from divertor region for radiative power dissipation to mitigate the q_{ot}, and the D-T discharge with impurity seeding should be investigated in future work.

3.2. The effect of D-T isotope on divertor neutral and radiation

To illustrate the impact of D-T isotope on the divertor plasma, the D-T discharge with 1:1 proportional mixture (no external puffing) are chosen. The ion density n_{D+} and n_{T+}, atomic density n_D and n_T, and molecular density n_{D2} and n_{T2}, along the outer divertor target are shown in Fig.4(a-c). It can be seen that at the 1:1 D-T discharge, both of T ion density and neutral density are higher than that of D. For the ion density, n_{D+} near separatrix is about 2.5 times than that of T. For neutral particles, the distribution differences between D and tritium T are mainly concentrated in the private flux region (PFR) and near the separatrix, where the n_T and n_{T2} are approximately 30% higher than those of D.

Figs. 4(d-e) show the ratios of n_{T+} to n_{D+}, and T neutral particle density to D neutral particle density in the divertor region, respectively. It can be observed that in the near SOL and the PFR, as the poloidal distance from the target decreases, the separation phenomenon between D and T becomes more pronounced.This phenomenon can be explained by the recycled atomic energy shown in Figs. 4(f-g): on one hand, the energy recycling coefficient of D is larger (as shown in Fig. 2(b)), and the D atoms obtained by reflection have a higher initial energy compared with T; on the other hand, the charge-exchange cross-section of D is larger (as shown in Fig. 2(d)), and the diffusion coefficient of isotopes can be estimated by the formula $D \approx \lambda_{CX} C_S \sim m^{-1/2}$ (where D denotes the diffusion coefficient, λ_{CX} is the charge-exchange mean free path; C_S is the atoms sound velocity; m is the isotope mass)[15]. The charge-exchange process further increases the energy of D atoms in the divertor, making them more likely transport to far from the target areas and be ionized. This leads to a decrease in the densities of D neutral particles, as well as n_{D+} in the divertor region, while their density are higher in the core region (as shown in Fig. 3(a)).

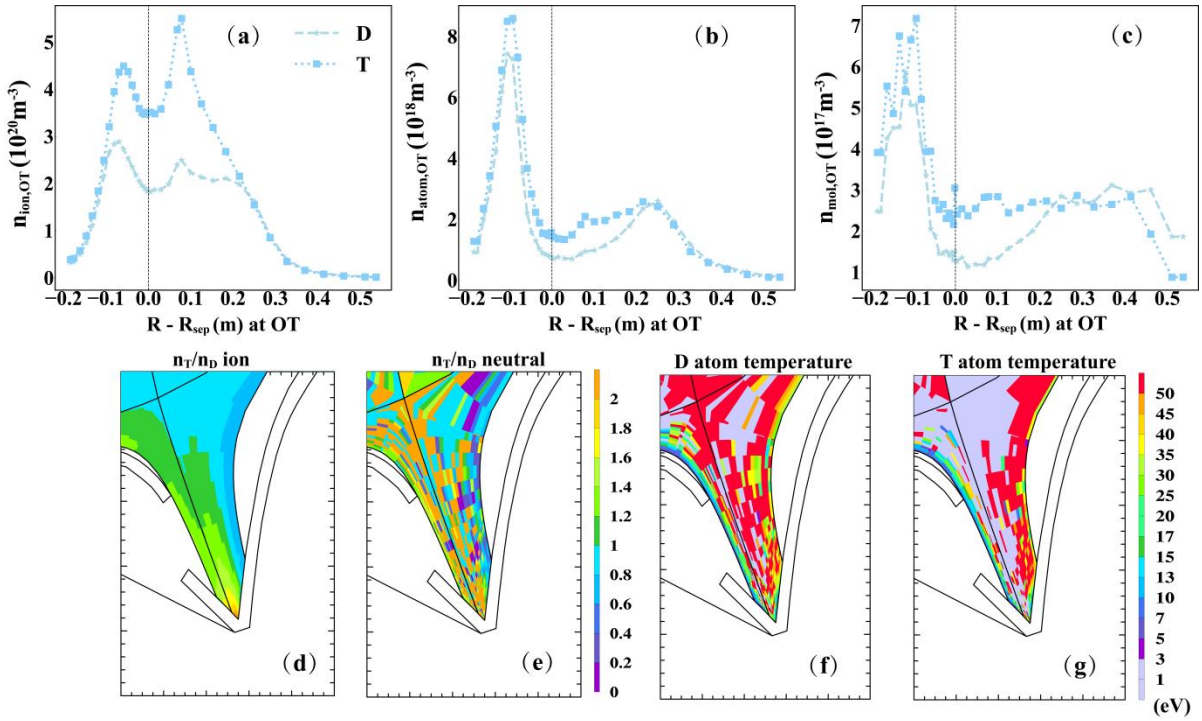

FIG.4 Profile of D and T (a) $n_{ion,OT}$, (b)$n_{atom,OT}$,(c) $n_{molecular,OT}$ at OT in different discharge conditions. And (d)n_{T+}/n_{D+},(d)$n_{T,neutral}/n_{D,neutral}$ ratio, (e-f) D and T atom temperature at the outer divertor region.

TABLE 2. The radiated power by D and T in different regions with different discharge conditions. Unit(MW).

Discharge condition	Outer divertor			Inner divertor			Upstream SOL+ Core		
	Total	D	T	Total	D	T	Total	D	T
D w/o puff	7.8	7.8	/	7.4	7.4	/	1.8	1.8	/
D+T w/o puff	9.1	3.8	5.3	8.5	4.0	4.5	1.8	0.9	0.9
D puff	8.5	8.5	/	8.0	8.0	/	1.9	1.9	/
D+T puff	10.7	4.5	6.2	10.4	4.9	5.5	2.0	1.0	1.0

In order to understand how the isotope effect promotes to achieve the lower q_t, the conservation of energy in the divertor is analyzed. The power radiation Q_{rad} is the energy loss due to particle radiate. In these cases, the Q_{rad} is mostly contribute by pure D or T radiation (including bremsstrahlung energy loss and neutral particle radiation), and the plasma surface recombination dissipation is very small so that it could be neglected. As shown in Table 2, the core region Q_{rad} is relatively small and may even be negative. Fuel puffing could increase Q_{rad} in the divertor region by approximately 10%. In D-T discharge, since T neutral are more concentrated in divertor, the Q_{rad} from T radiation is about 40% higher than that from D radiation. Additionally, the Q_{rad} of D-T discharge is 20% higher than that of D discharge. Therefore, the isotope effect of D-T can lead to a significant decrease in q_t .

4. CONCLUSION

In this work, the effect of D-T isotope on CFEDR device deposition power of target, with GW heating power discharge has been studied by SOLPS-ITER simulation. Four cases are considered: pure D discharge (no external puffing); D-T discharge with 1:1 proportional mixture (no external puffing); pure D discharge (D injected rate is 2×10^{22} s^{-1} from the upper puffing port); D-T 1:1 discharge with proportional mixture (both D and T injected rate is 1×10^{22} s^{-1} from the upper puffing port). The simulation results show that regardless of the presence of external puffing, the outer mid-plane electron density of the D-T discharg is larger at the separatrix, as well as wider heat flux decay length, which is qualitatively consistent with both experiments and simulations of JET D-T discharges. Fuel gas puffing at the upstream effectively reducing $T_{e,ot}$ and $q_{ot.}$ In the D-T discharge condition, both $T_{e,ot}$ and q_{ot} decrease by 15%. The T ion density and T neutral density are higher than that of D in D-T discharge, which could be explained by the recycled atom and charge-exchange collisions: on one hand, the energy recycling coefficient of D is larger , and the D atoms obtained by reflection have a higher initial energy compared with T; on the other hand, the charge-exchange cross-section of D is larger, further increases the energy of D atoms in the divertor, making them more likely transport to far from the target areas and be ionized. This leads to a decrease in the densities of D neutral particles, as well as n_{D+} in the divertor region. Since T neutral are more concentrated in divertor, the radiation from T radiation is higher than that from D radiation. Additionally, Therefore, the isotope effect of D-T can lead to a significant decrease in q_t .

ACKNOWLEDGEMENTS

This work is supported by National Natural Science Foundation of China under Grant Nos. 12405252, 12122503, 12235002, 12261131496, China Postdoctoral Science Foundation Nos.2024M750305.

REFERENCES

[1] Pitts R A et al 2019 *Nucl. Mater. Energy* **20** 100696

[2] Ding R et al 2025 *Plasma Sci. Technol.*
[3] Makarov S O et al 2021 *Phys. Plasmas* **28** 062308
[4] Grogin N A and Kocevski D D 1997 *Plasma Phys. Control. Fusion* **39** B103–B114
[5] Maslov M et al 2023 *Nucl. Fusion* **63** 112002
[6] Faitsch M et al 2023 *Nucl. Fusion* **63** 112013
[7] Sun H J et al 2023 *Nucl. Fusion* **63** 016021
[8] Bonnin X et al 2016 *Plasma Fusion Res.* **11** 1403102
[9] Kaveeva E et al 2023 *Contrib. to Plasma Phys.* e202300118
[10] Makarov S O et al 2023 *Nucl. Fusion* **63** 026014
[11] Zhang C et al 2019 *Plasma Phys. Control. Fusion* **61** 115013
[12] Sawada K and Fujimoto T 1995 *J. Appl. Phys.* **78** 2913–24
[13] Reiter D 2011 *The data file AMJUEL : Additional Atomic and Molecular Data for EIRENE*
[14] Reiter D 1987 *The data file HYDHEL : Atomic and Molecular Data for EIRENE based upon : Janev , Langer , Evans , Post , " Elementary Processes in Hydrogen-Helium Plasmas "*
[15] Li Q et al 2025 *Nucl. Fusion* **65** 026069